Mitochondrial [4Fe-4S] protein assembly involves reductive [2Fe-2S] cluster fusion on ISCA1–ISCA2 by electron flow from ferredoxin FDX2

Benjamin Dennis Weiler[a], Marie-Christin Brück[a], Isabell Kothe[a], Eckhard Bill[b], Roland Lill[a,c,1], and Ulrich Mühlenhoff[a,1]

[a]Institut für Zytobiologie und Zytopathologie, Philipps-Universität Marburg, 35032 Marburg, Germany; [b]Max-Planck-Institut für Chemische Energiekonversion, 45470 Mülheim an der Ruhr, Germany; and [c]LOEWE Zentrum für Synthetische Mikrobiologie SYNMIKRO, 35043 Marburg, Germany

Edited by Elizabeth Anne Craig, University of Wisconsin, Madison, WI, and approved July 16, 2020 (received for review March 2, 2020)

The essential process of iron-sulfur (Fe/S) cluster assembly (ISC) in mitochondria occurs in three major phases. First, [2Fe-2S] clusters are synthesized on the scaffold protein ISCU2; second, these clusters are transferred to the monothiol glutaredoxin GLRX5 by an Hsp70 system followed by insertion into [2Fe-2S] apoproteins; third, [4Fe-4S] clusters are formed involving the ISC proteins ISCA1–ISCA2–IBA57 followed by target-specific apoprotein insertion. The third phase is poorly characterized biochemically, because previous in vitro assembly reactions involved artificial reductants and lacked at least one of the in vivo-identified ISC components. Here, we reconstituted the maturation of mitochondrial [4Fe-4S] aconitase without artificial reductants and verified the [2Fe-2S]-containing GLRX5 as cluster donor. The process required all components known from in vivo studies (i.e., ISCA1–ISCA2–IBA57), yet surprisingly also depended on mitochondrial ferredoxin FDX2 and its NADPH-coupled reductase FDXR. Electrons from FDX2 catalyze the reductive [2Fe-2S] cluster fusion on ISCA1–ISCA2 in an IBA57-dependent fashion. This previously unidentified electron transfer was occluded during previous in vivo studies due to the earlier FDX2 requirement for [2Fe-2S] cluster synthesis on ISCU2. The FDX2 function is specific, because neither FDX1, a mitochondrial ferredoxin involved in steroid production, nor other cellular reducing systems, supported maturation. In contrast to ISC factor-assisted [4Fe-4S] protein assembly, [2Fe-2S] cluster transfer from GLRX5 to [2Fe-2S] apoproteins occurred spontaneously within seconds, clearly distinguishing the mechanisms of [2Fe-2S] and [4Fe-4S] protein maturation. Our study defines the physiologically relevant mechanistic action of late-acting ISC factors in mitochondrial [4Fe-4S] cluster synthesis, trafficking, and apoprotein insertion.

iron-sulfur cluster | late-acting ISC factors | cellular thiol-redox systems | monothiol glutaredoxin

Proteins with iron-sulfur (Fe/S) cofactors play important roles in fundamental cellular processes, including redox reactions, catalysis, translation, DNA synthesis and repair, antiviral defense, and the sensing of environmental conditions (1). The biogenesis of Fe/S proteins is catalyzed by complex, conserved assembly systems (2–6). In eukaryotes including humans, maturation is initiated in mitochondria by the iron-sulfur cluster assembly (ISC) machinery, and for extramitochondrial Fe/S proteins additionally requires the cytosolic Fe/S protein assembly system (7). The mitochondrial pathway occurs in three major steps involving 18 known proteins of mostly bacterial origin. First, a [2Fe-2S] cluster is formed de novo on the scaffold protein ISCU2 by the cysteine desulfurase complex NFS1–ISD11–ACP1, frataxin, and the mitochondrial [2Fe-2S] ferredoxin FDX2 (8–10). While fungi and many unicellular eukaryotes contain a single ferredoxin (termed Yah1) for this task, mitochondria from humans and other vertebrates harbor two. FDX1 (also known as adrenodoxin) is specific for steroid biosynthesis, while FDX2 is essential for [2Fe-2S] cluster synthesis on ISCU2 by the NFS1 complex (8, 9, 11). Whether FDX1 also contributes to Fe/S protein biogenesis is under debate (2). Whether mitochondrial FDX2 is also required in later steps of the ISC machinery is unknown and, due to its initial involvement in early steps of Fe/S cluster synthesis, difficult to address in vivo.

In the second step, the newly assembled [2Fe-2S] cluster on ISCU2 is transferred to the monothiol glutaredoxin GLRX5, a reaction requiring the mitochondrial Hsp70 chaperone HSPA9 and its dedicated J-type cochaperone HSC20 (2–4, 12). Dimers of monothiol glutaredoxins, including GLRX5, transiently bind a bridging [2Fe-2S] cluster that can be further transferred to [2Fe-2S] apoproteins in vitro (13–16). Low levels of GLRX5 result in severe defects of all cellular Fe/S proteins and cause fatal human disease (17–21). This suggests that mitochondrial GLRX5 plays a decisive role in Fe/S protein biogenesis, potentially as a Fe/S cluster transfer factor.

In the third step, the [2Fe-2S] cluster is converted into a [4Fe-4S] cluster type, a reaction involving the A-type ISC proteins ISCA1–ISCA2 and the interacting IBA57 (22–28). For some Fe/S proteins, such as complex I and lipoyl synthase, additional specific Fe/S cluster-targeting factors are implicated, such as IND1 (also known as NUBPL1), NFU1, and BOLA3 (2). Mutations in all of these late-acting ISC factors cause the "multiple mitochondrial dysfunction syndromes," with severe, often lethal outcome due to defects in mitochondrial [4Fe-4S] proteins, documenting the importance of these factors for viability (29–34).

Significance

Synthesis of iron-sulfur clusters (ISC) and their insertion into apoproteins in eukaryotes requires the conserved, essential mitochondrial ISC and cytosolic Fe/S protein assembly machineries. Genetic mutations in most of the 18 different human ISC genes cause neurological, metabolic, and hematological diseases with often lethal outcome. Here, we have biochemically reconstituted the least-understood part of mitochondrial iron-sulfur protein assembly: The synthesis and insertion of [4Fe-4S] clusters. Apart from the in vivo-identified ISC factors (i.e., the [2Fe-2S] cluster donor GLRX5 and ISCA1–ISCA2–IBA57), this reaction specifically requires reduced ferredoxin FDX2, but not FDX1, for reductive fusion of $[2Fe\text{-}2S]^{2+}$ into $[4Fe\text{-}4S]^{2+}$ clusters. In contrast, [2Fe-2S] cluster transfer from GLRX5 to [2Fe-2S] target proteins occurs rapidly without any additional ISC factor.

Author contributions: B.D.W., M.-C.B., E.B., R.L., and U.M. designed research; B.D.W., M.-C.B., I.K., E.B., and U.M. performed research; B.D.W., M.-C.B., I.K., E.B., and U.M. analyzed data; and R.L. and U.M. wrote the paper.

The authors declare no competing interest.

This article is a PNAS Direct Submission.

[1]To whom correspondence may be addressed. Email: Lill@staff.uni-marburg.de or muehlenh@staff.uni-marburg.de.

This article contains supporting information online at https://www.pnas.org/lookup/suppl/doi:10.1073/pnas.2003982117/-/DCSupplemental.

First published August 12, 2020.

The mechanism underlying the conversion of [2Fe-2S] into [4Fe-4S] clusters by late-acting ISC factors is poorly defined biochemically. Consistent with the genetic interaction of yeast *ISA1* and *ISA2* with *GRX5* (35), human GLRX5 was shown to interact with and transfer [2Fe-2S] clusters to ISCA1 and ISCA2 in vitro, suggesting that GLRX5 might be the cluster donor for formation of [4Fe-4S] proteins (15, 25, 26, 36). Furthermore, A-type ISC proteins have been assigned as Fe/S cluster "fusion," "transfer," or "carrier" proteins on the basis that they can accommodate [2Fe-2S] and [4Fe-4S] clusters and transfer them to apoproteins in vitro, yet all of these reactions typically depended on the presence of DTT (15, 25, 26, 28, 37, 38). Hence, the mechanism and site of [4Fe-4S] cluster formation by these proteins remains largely unresolved. Moreover, the relative functional importance of ISCA1, ISCA2, and IBA57 for mitochondrial [4Fe-4S] proteins biogenesis is a matter of debate. In *Saccharomyces cerevisiae*, deletion of *ISA1*, *ISA2*, or *IBA57* genes elicit identical phenotypes of a general mitochondrial [4Fe-4S] protein deficiency, indicating that each of these ISC proteins plays a specific, indispensable role in this process (22, 23). This is consistent with the RNAi-mediated depletion of each of these three proteins in HeLa cells resulting in a general deficiency in mitochondrial [4Fe-4S] protein function (24). In marked contrast, shRNA-assisted knockdown in mouse suggested that ISCA1 alone might be sufficient for mitochondrial [4Fe-4S] protein biogenesis in skeletal muscle and neuronal cells (25). The opposite conclusion was reached by in vitro studies with human ISC proteins, suggesting the requirement of only GLRX5, ISCA2, and IBA57 for [4Fe-4S] protein maturation (26). Resolving the question whether these proteins function together or alone, and whether they work as Fe/S cluster fusion, transfer, carrier, or targeting factor, or even as an enzyme critically depends on faithful reconstitution of the in vivo pathway.

Here, we present insights into the biochemical mechanisms of [2Fe-2S] and [4Fe-4S] protein assembly in mitochondria. We developed an in vitro reconstitution system to test the function of potentially involved ISC factors, yet avoiding artificial reductants. We surprisingly found that, in addition to the expected cluster donor GLRX5 and ISCA1–ISCA2–IBA57 proteins, the reduced ferredoxin FDX2 was essential for [4Fe-4S] cluster assembly on aconitase. FDX2 was shown to transfer electrons to ISCA1–ISCA2 for reductive $[2Fe\text{-}2S]^{2+}$ to $[4Fe\text{-}4S]^{2+}$ cluster fusion. Apparently, the ferredoxin requirement has been missed in previous in vivo and in vitro studies. We further compare the final step of [4Fe-4S] protein maturation with that of [2Fe-2S] protein assembly and disclose characteristic similarities and differences of these reactions.

Results

Critical Reassessment of Protocols for [4Fe-4S] Protein Maturation by [2Fe-2S] Donors. Virtually all published [4Fe-4S] protein maturation protocols include the artificial thiol reductant DTT. Despite this, it is unknown whether and why this compound is needed, and what its potential physiological counterpart may be. Since the mitochondrial monothiol glutaredoxin GLRX5, based on in vivo and in vitro findings, likely plays a central role in Fe/S cluster trafficking to apoproteins, we addressed its role as a potential [2Fe-2S] cluster donor for in vitro maturation of [4Fe-4S] proteins (13, 14, 39). Consistent with previous findings for several [2Fe-2S] cluster-bearing ISC proteins (13, 14, 25, 26, 28, 36, 40–44), the [2Fe-2S] cluster of GLRX5 was transferred and converted into a [4Fe-4S] cluster on human mitochondrial aconitase ACO2 or the yeast cytosolic aconitase-type Leu1 in the presence of DTT (Fig. 1 *A* and *B*). Leu1's isopropylmalate isomerase enzyme activities increased further when the apoprotein was reduced by TCEP immediately prior to the assay, indicating that Fe/S cluster insertion benefits from thiol reduction of target apoproteins (Fig. 1 *B*, *Right*). However, in the absence of DTT, hardly any maturation of ACO2 or Leu1 by GLRX5 occurred (Fig. 1 *A* and *B*). DTT could be replaced only partially by other strong chemical thiol reductants, such as TCEP or β-mercaptoethanol, indicating that disulfide reduction of the target apoproteins is not the main reason for the poor maturation efficiency without DTT. In line with this, the physiological thiol-specific redox system consisting of glutathione (GSH) plus dithiol glutaredoxin Glrx1 did not support maturation of ACO2 or Leu1 (Fig. 1 *A* and *B*).

Successful maturation of aconitase-type [4Fe-4S] proteins has been reported previously using the [2Fe-2S] holo-forms of the mitochondrial A-type ISC proteins ISCA1, ISCA2, or their bacterial counterparts as cluster donors, yet these reactions, too, always contained DTT (20, 25, 26, 28, 36, 37, 40). In the presence of the physiological Glrx1-GSH reducing system (i.e., no added DTT), hardly any maturation of ACO2 or Leu1 was observed with reconstituted human holo-ISCA1 or holo-ISCA2 (Fig. 1*C*). A similar finding was made for chemically coreconstituted holo-ISCA1–ISCA2, even in the presence of human IBA57 (i.e., all three ISC factors known to be essential for in vivo ACO2 assembly) (22–24). Clearly, these findings indicate that the transfer of [2Fe-2S] clusters and their conversion into [4Fe-4S] clusters for insertion into aconitase-like proteins in vitro was assisted by DTT rather than the ISC proteins. This nonphysiological DTT function was different from its thiol-reducing activity, since it could not be replaced by artificial or physiological thiol reducing systems.

An Essential Role of Mitochondrial FDX2 in the Maturation of Aconitase. Since neither GLRX5 nor ISCA1–ISCA2–IBA57 supported the assembly of [4Fe-4S] proteins, we tried the combined addition of these ISC factors to fulfill the known in vivo requirements for [4Fe-4S] aconitase maturation (22–24). However, upon incubation of holo-GLRX5 (50 μM) with catalytic amounts of coreconstituted ISCA1–ISCA2–IBA57 (5 μM each), we still obtained a rather low efficiency of ACO2 maturation in the presence of the Glrx1-GSH system (Fig. 2*A*, first bar). We therefore reasoned that our reconstitution reaction lacks a further essential assembly factor. The conversion of two oxidized low-potential $[2Fe\text{-}2S]^{2+}$ clusters into an oxidized low-potential $[4Fe\text{-}4S]^{2+}$ cluster as found on aconitase-type proteins formally requires the input of two electrons. Hence, a possible explanation for the failure to efficiently mature ACO2 may be the lack of a reducing factor (45). Since Glrx1-GSH apparently did not fulfill this task, we tested the mitochondrial ferredoxin FDX2 together with its cognate ferredoxin reductase (FDXR) and NADPH. When holo-GLRX5 (50 μM) and apo-ACO2 (20 μM) were mixed with catalytic quantities (10% relative to GLRX5) of chemically coreconstituted holo-ISCA1–ISCA2 plus IBA57 and FDX2–FDXR–NADPH, efficient Fe/S cluster transfer to and maturation of ACO2 (more than 60% after 10 min) was observed as estimated by aconitase enzyme activity (Fig. 2*A*, second bar). Maturation reached completion within 10 min (Fig. 2*B*). As a control, omission of either GLRX5, holo-ISCA1–ISCA2, IBA57, or the electron transfer chain FDX2–FDXR–NADPH lead to hardly any ACO2 maturation (Fig. 2 *A* and *B*). The dependence on any of these ISC components, including those known to be required in vivo (ISCA1–ISCA2–IBA57), suggested that this in vitro reaction closely mimics the physiological situation. Moreover, the almost quantitative maturation of ACO2 and the high specific activities (significantly higher than upon reconstitution with DTT) (compare with Fig. 1*A*) indicate that holo-GLRX5, and not the catalytic amounts of holo-ISCA1–ISCA2, ultimately served as the Fe/S cluster donor for ACO2 maturation. Interestingly, the catalytic function of ISCA1–ISCA2 depended on their prior coreconstitution of an Fe/S cluster on the heterodimer. When the reconstituted holo-ISCA1–ISCA2 complex was replaced by equal catalytic amounts of apo-ISCA1 and apo-ISCA2, only background maturation of ACO2 was observed (Fig. 2*C*). The same was seen for separately reconstituted holo-ISCA1 and holo-ISCA2 added in catalytic amounts, either separately or combined.

Having a working reconstitution system at hand, we asked whether the holo-ISCA1–ISCA2 complex can replace GLRX5 as

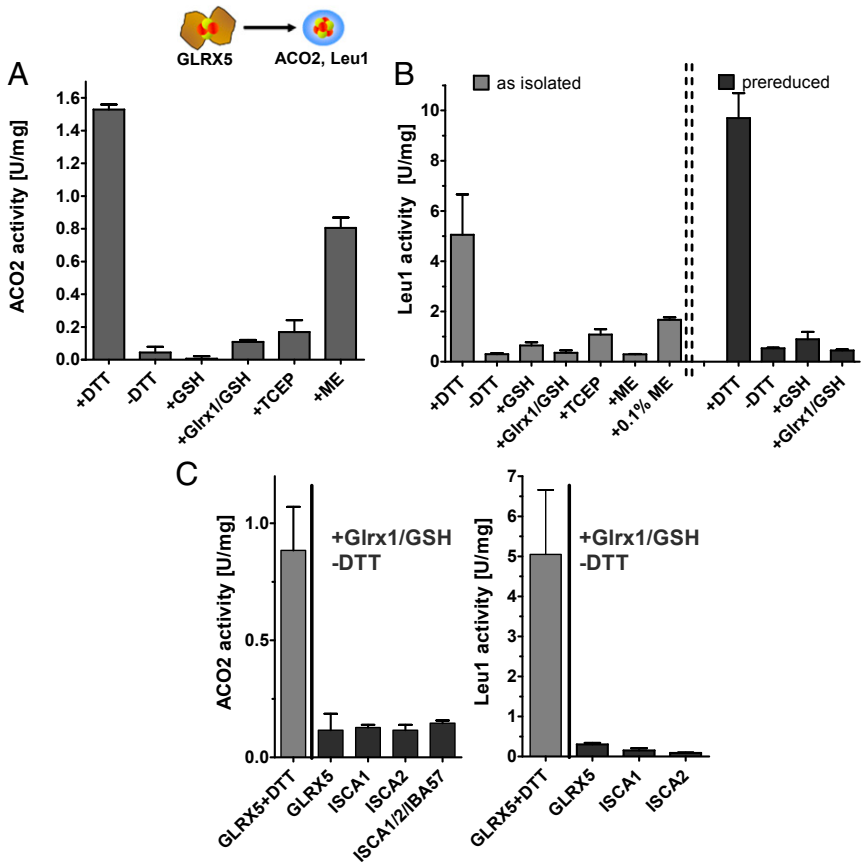

Fig. 1. Unassisted maturation of aconitase-like [4Fe-4S] proteins by [2Fe-2S] cluster transfer from GLRX5 requires thiol reductants. Human holo-GLRX5 (50 μM) was incubated with human apo-ACO2 (20 μM) (*A*) or yeast apo-Leu1 (20 μM) (*B*) for 10 min in the presence or absence of 2 mM DTT, 4 mM GSH, 4 mM GSH plus 25 μM mouse Glrx1 (Glrx1/GSH), 4 mM TCEP, or 4 mM β-mercaptoethanol (ME). Fe/S cluster transfer was estimated by measuring ACO2 or Leu1 enzyme activities. In *B*, apo-Leu1 was either used as isolated (*Left*) or was reduced by 10 mM TCEP anaerobically in situ immediately prior utilization (prereduced; *Right*). (*C*) Fe/S cluster transfer to and assembly of human ACO2 (20 μM; *Left*) or apo-Leu1 (20 μM; *Right*) from the indicated chemically reconstituted human holo-ISC proteins (50-μM each) were performed and estimated as above in the presence of Glrx1/GSH (dark gray bars). Control reactions with GLRX5 as cluster donor in the presence of DTT are included (gray bars). Error bars indicate the SEM ($n \geq 3$).

a cluster donor when added in stoichiometric rather than catalytic amounts relative to apo-ACO2. No significant maturation was observed under these conditions despite the presence of the FDX2 electron transfer chain, supporting the conclusion that GLRX5 is the cluster donor in this in vitro reaction (Fig. 2*D*). Despite their importance for the overall maturation process, the Fe/S clusters present on holo-ISCA1–ISCA2 could not be used successfully for ACO2 assembly, in contrast to what has been described for A-type ISC proteins in the presence of DTT (25, 26, 28, 36, 37). This result clearly indicates that the ISCA1–ISCA2 proteins, like IBA57, perform a catalytic role in the reductive conversion of the GLRX5-bound $[2Fe\text{-}2S]^{2+}$ to a $[4Fe\text{-}4S]^{2+}$ cluster.

No Crucial In Vivo Role of NFU1 in Aconitase Maturation. We next asked whether our assay lacks further ISC components and focused on the late-acting ISC factor NFU1. Conflicting results have been obtained for the requirement of NFU1 in aconitase maturation in vivo. While yeast cells lacking Nfu1 show a two- to fivefold lower aconitase activity, human cell lines depleted in NFU1 or patient cells lacking NFU1 display normal aconitase levels (29, 30, 46–48). Consistent with a role in aconitase maturation and with earlier in vitro experiments (49–51), chemically reconstituted human holo-NFU1 efficiently activated apo-ACO2, yet only in the presence of reductants (*SI Appendix*, Fig. S1*A*). Using our in vitro reconstitution system, the inclusion of catalytic amounts of apo-NFU1 (20% of apo-ACO2) increased the efficiency of ACO2 maturation slightly (15%) (Fig. 2*E*). These in vitro data suggest a role of human NFU1 in [4Fe-4S] cluster transfer to aconitase.

The question remained why the lack of human NFU1 is not associated with an aconitase defect in cultured and patient cells, and what may explain the difference to yeast cells. We therefore investigated whether the in vivo aconitase defect upon yeast *NFU1* deletion could be an at least partially indirect phenotype. *nfu1Δ* cells are severely impaired in SDH and lipoyl synthase (Lip5) activities, thereby impacting respiration and several lipoylated TCA cycle-related enzymes (47, 48). Decreased respiration and an interrupted TCA cycle might indirectly affect aconitase function. To check this idea, we compared the aconitase activity in *nfu1Δ* cells with that of cells lacking Lip5 (*lip5Δ*). Strikingly, the deletion of *LIP5* phenocopied the deletion of *NFU1*, as indicated by a fivefold lower aconitase activity in both cells compared to wild-type (Fig. 2*F*). This finding shows that an impaired TCA cycle indeed severely affects aconitase function in yeast, suggesting that the aconitase defect in *nfu1Δ* cells may at least in part be indirect. This notion was further supported by the analysis of a constitutively expressed mitochondria-targeted Leu1 (an aconitase-type enzyme) in *nfu1Δ* cells. Leu1 has been shown earlier to be a bona fide substrate of the ISC system when imported into mitochondria (52), and as expected for a mitochondrial [4Fe-4S] protein, its maturation and activity fully depended on Iba57 function (Fig. 2*G* and *SI Appendix*, Fig. S1*B*). In contrast, *nfu1Δ* cells showed wild-type activity of this mitochondrial

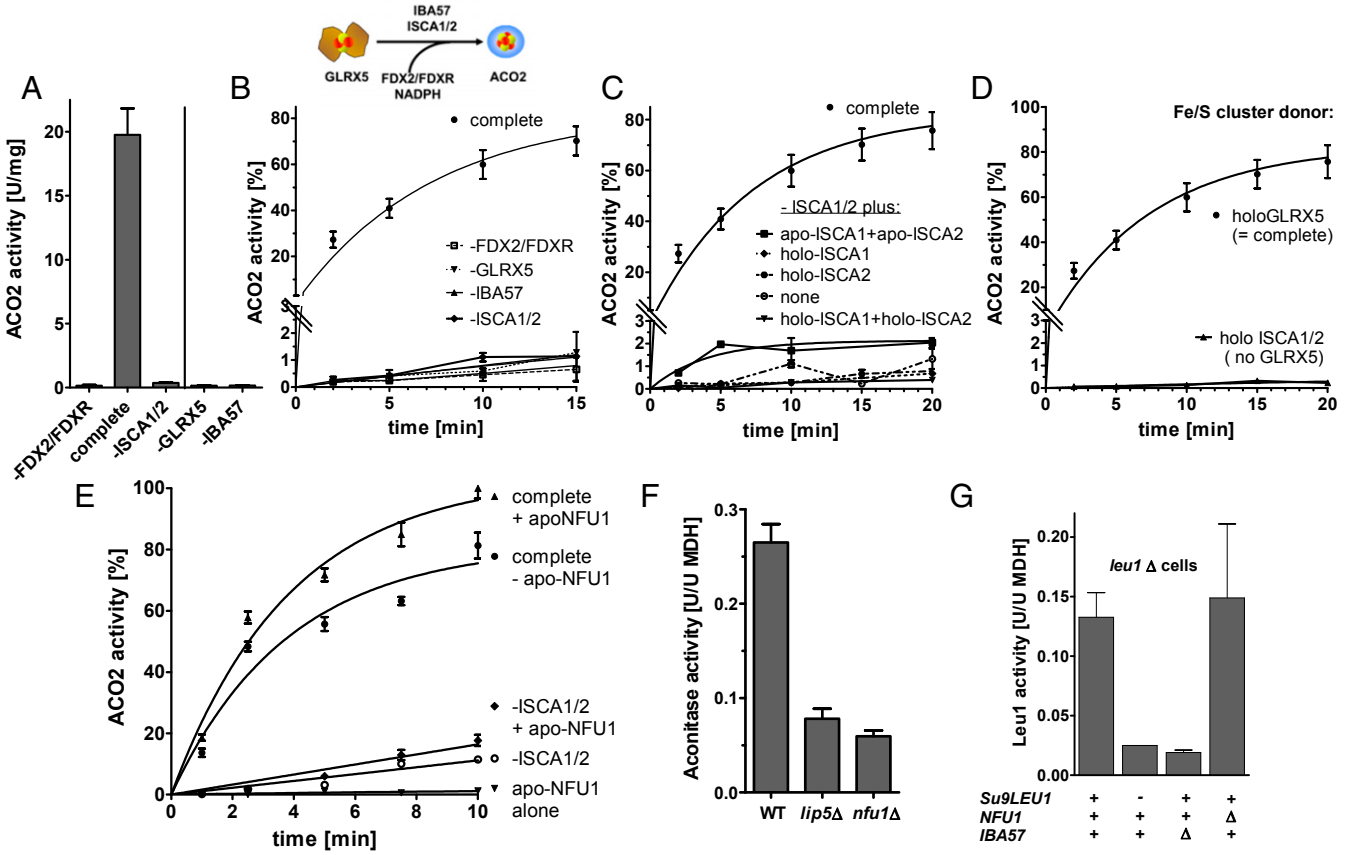

Fig. 2. Maturation of [4Fe-4S] aconitase requires GLRX5 as cluster donor, catalysis by late ISC factors, and the ferredoxin FDX2. Fe/S cluster transfer from human holo-GLRX5 (50 μM) to apo-ACO2 (20 μM) in the presence of coreconstituted ISCA1–ISCA2 complex (ISCA1/2), IBA57, FDX2 (5 μM each), FDXR (1 μM), 1 mM NADPH, 4 mM GSH, and 25 μM Glrx1 (complete). Where indicated, individual ISC components were omitted from the complete reaction. (*A*) Aconitase activities determined after 10 min. (*B*) Time course of aconitase activation. (*C*) The coreconstituted ISCA1–ISCA2 complex (ISCA1/2) was replaced by the indicated ISCA1 or ISCA2 species. All other components were present as in the complete reaction (see *A*). (*D*) Aconitase activation was performed as in *B* with holo-GLRX5 or with coreconstituted ISCA1/2 complex (50 μM each) as alternative Fe/S cluster donors. (*E*) Aconitase activation was performed as in *B* (complete) in the presence or absence of apo-NFU1 (5 μM). Reactions lacking ISCA1/2 and a transfer from apo-NFU1 alone are included as controls. Solid lines represent fits of the data according to a pseudofirst order kinetics. Maximum aconitase activity was 20 U/mg (*A–D*) and 9 U/mg (*E*). Error bars indicate the SEM ($n \geq 3$). (*F*) Aconitase activities were measured in cell extracts of BY4742 wild-type and isogenic *lip5*Δ and *nfu1*Δ cells. (*G*) Leu1 activities of cell extracts from BY4742 *leu1*Δ/*iba57*Δ and *leu1*Δ/*nfu1*Δ cells that express a mitochondria-targeted Su9-Leu1 as indicated. Error bars indicate the SEM ($n \geq 4$).

aconitase-type enzyme. In sum, our findings now provide a consistent picture for the involvement of NFU1 in aconitase maturation in yeast or human cells. It appears that NFU1 at best performs an auxiliary role in aconitase maturation, and its potential function can readily be bypassed in living cells.

FDX1 Cannot Replace FDX2 in Its Role in Aconitase Maturation. We next asked whether successful in vitro ACO2 maturation specifically required FDX2, or whether it could be replaced by other cellular electron donor systems. We first tested the human mitochondrial ferredoxin FDX1 (also known as adrenodoxin), which is closely related to FDX2, yet shows high specificity for steroid biosynthesis (11, 53). When FDX1 was used instead of FDX2, virtually no maturation of ACO2 occurred (Fig. 3). In contrast, efficient activation of ACO2 was observed when the mitochondrial ferredoxin Yah1 from the thermophilic fungus *Chaetomium thermophilum* (CtYah1) was used. Like most eukaryotes, this fungus possesses only a single mitochondrial ferredoxin. When FDX2–FDXR was replaced by mitochondrial TRX2 and its cognate thioredoxin reductase (Trr2), virtually no activation of ACO2 was observed. Similarly, Glrx1-GSH was inefficient (Fig. 1 *C*, *Left*), demonstrating that these two physiological thiol-specific redox systems are incapable of mediating the reductive coupling of $[2Fe\text{-}2S]^{2+}$ into $[4Fe\text{-}4S]^{2+}$ clusters. Moreover, no ACO2 activation was seen, when FDX2–FDXR–NADPH were replaced by 50 μM Fe^{2+} and excess ascorbic acid, a condition that allows conversion of aconitase carrying an oxidized $[3Fe\text{-}4S]^{+}$ cluster into an active $[4Fe\text{-}4S]^{2+}$ protein (54). Taken together, our data identify the so far undiscovered requirement of the mitochondrial electron transfer chain FDX2–FDXR–NADPH for the reductive coupling of $[2Fe\text{-}2S]^{2+}$ clusters during the terminal step of [4Fe-4S] protein assembly.

Physical Interactions of Mitochondrial Ferredoxin with Late ISC Factors. In order to identify the electron acceptor of mitochondrial FDX2 in ACO2 maturation, we searched for the interaction partners of FDX2 within the late-acting ISC system. First, we carried out coimmunoprecipitation experiments using detergent lysates of mitochondria isolated from various *S. cerevisiae* strains. Galactose-inducible *GAL1-10* promoter exchange cells for *GRX5*, *ISA1*, *ISA2*, *IBA57*, and *YAH1* were cultivated in galactose-containing medium to overproduce the respective gene products. Coimmunoprecipitation was performed using specific antibodies against either Grx5 or the yeast ferredoxin Yah1 (55). We found that α-Grx5 antibodies coprecipitated Yah1 from Gal-*YAH1* mitochondrial extracts (*SI Appendix*, Fig. S2). This coimmunoprecipitation

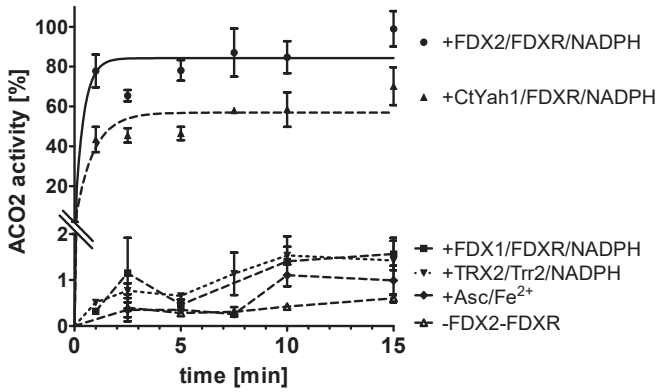

Fig. 3. FDX1 cannot replace FDX2 function in the maturation of [4Fe-4S] aconitase. Fe/S cluster transfer from human holo-GLRX5 (50 μM) to apo-ACO2 (20 μM) was performed as in Fig. 2 in the presence of coreconstituted ISCA1-ISCA2 complex and IBA57. As reducing systems we used: (•) FDX2 (5 μM), FDXR (1 μM), and 1 mM NADPH; (■) FDX1 (5 μM), FDXR (1 μM), and 1 mM NADPH; (▲) CtYah1 (5 μM), FDXR (1 μM), and 1 mM NADPH; (▼) TRX2 (5 μM), Trr2 (0.5 μM), and 1 mM NADPH; or (♦) 1 mM ascorbate and 50 μM $FeCl_2$. A control without FDX2-FDXR is also added (△). The upper two curves represent fits of the data according to a pseudofirst order kinetics. Maximum aconitase activity was 9 U/mg.

was specific, because hardly any Yah1 was seen with beads coupled with a nonspecific serum. Furthermore, no Yah1 signal was observed when α-Grx5 immunobeads were incubated in buffer alone. No positive results were obtained for other potential pairwise interactions, because Grx5- or Yah1-specific antisera failed to coimmunoprecipitate Isa1, Isa2, or Iba57 from any of the strains tested.

Next, we studied bimolecular interactions in vitro by Bio-layer interferometry (BLI). For this approach, we chose purified recombinant ISC proteins from *C. thermophilum*, since they are fairly oxygen-resistant in reconstituted holo-forms. The ferredoxin CtYah1 was labeled with biotin, immobilized on streptavidin sensors, and subjected to binding studies in parallel with empty sensors. Signals from the latter detection were subtracted in order to correct for unspecific binding. Advantageously, BLI allowed the interaction analysis of all combinations of reduced or oxidized CtYah1 and apo- or holo-CtGrx5. Consistent with the in vivo findings above, immobilized CtYah1 interacted with CtGrx5. However, an interaction was seen only for oxidized CtYah1 and apo-CtGrx5 (K_D ~ 200 μM), and particularly not for reduced CtYah1 and holo-CtGrx5 (i.e., the functionally relevant combination for productive electron transfer) (Fig. 4*A* and *SI Appendix*, Fig. S3 and Table S1). While these observations are consistent with the in vivo immunoprecipitation studies above (carried out under nonreducing conditions and in the presence of oxygen, conditions that likely destroy the labile Fe/S clusters on Grx5), the interaction of apo-Grx5 with reduced Yah1 does not suggest any role in electron transfer.

We therefore investigated the interaction of CtYah1 with the ISCA homologs from *C. thermophilum*, CtIsa1 and CtIsa2. First, we studied the interaction with a chemically coreconstituted holo-CtIsa1–CtIsa2 (CtIsa1/2) complex, because this heterocomplex supported ACO2 maturation (compare with Fig. 2). Indeed, CtYah1 bound to holo-CtIsa1–CtIsa2, and this interaction was specific, as it was only seen with reduced CtYah1 (Fig. 4*B*). From concentration variation experiments, a dissociation constant K_D = 2.2 ± 0.6 μM was estimated (*SI Appendix*, Fig. S4). Thus, reduced CtYah1 interacts 100-fold stronger with CtIsa1–CtIsa2 than with apo-CtGrx5. In order to address whether this interaction requires the presence of Fe/S clusters on the Isa proteins, we studied the CtYah1 interaction with CtIsa2, which is much more stable than CtIsa1 in both the apo- and holo-forms. Both apo- and holo-CtIsa2 interacted with reduced CtYah1, yet the affinity of reduced CtYah1 for holo-CtIsa2 (K_D = 1.6 ± 0.3 μM) was approximately threefold higher than that for apo-CtIsa2 (K_D = 5.2 ± 0.7 μM) (Fig. 4 *C* and *D* and *SI Appendix*, Fig. S5 and Table S1). The same preference for holo-CtIsa2 was seen for oxidized CtYah1 (holo: K_D = 1.1 ± 0.3 μM; apo: 3.9 ± 0.8 μM). Taken together, the results of this binary interaction study provide ample evidence for a specific interplay of mitochondrial ferredoxin with the late ISC assembly factors. The strong preference of reduced CtYah1 for the Isa proteins rather than Grx5, its higher affinity for their holo-forms, and the strong preference for the heterodimeric holo-CtIsa1–CtIsa2 point toward holo-CtIsa1–CtIsa2 as the site of electron input from mitochondrial ferredoxin.

FDX2 Transfers Electrons to Holo-ISCA1–ISCA2 for IBA57-Dependent [2Fe-2S] Cluster Fusion. We sought to better understand the details of FDX2-mediated electron transfer requirement, and followed this reaction by UV/Vis spectrometry measuring the FDXR–FDX2-catalyzed oxidation of NADPH upon incubation with reconstituted holo-ISCA–ISCA2. An initial small absorption drop at 340 nm was observed, indicative of NADPH consumption, yet only little further decrease occurred at later times (Fig. 5*A* and *SI Appendix*, Fig. S6*A*). Since the extent of this absorption decay was far less than that expected for complete reduction of the entire 50 μM holo-ISCA1–ISCA2 by NADPH, this finding indicated that FDX2–FDXR–NADPH were not able to efficiently transfer electrons to holo-ISCA1–ISCA2. Strikingly, when we then added catalytic amounts of IBA57 (3 μM), a robust, continuous absorption decay at 340 nm with a half-life of 16 min was observed (Fig. 5 *A* and *B* and *SI Appendix*, Fig. S6). After 1 h ~60 μM NADPH was consumed (assuming that the absorption decay at 340 nm was solely due to NADPH oxidation).

The FDX2-catalyzed reaction was accompanied by spectral changes in the 400- to 700-nm range that represent the [2Fe-2S] cluster (see below) bound to ISCA1–ISCA2 (Fig. 5*A*). The difference spectrum (obtained by subtracting the spectrum recorded after 1-h incubation from that before initiation of electron transfer [start minus end]) showed a strong absorption decrease of the [2Fe-2S] cluster-specific peaks at 527 and 600 nm, but only a minor drop of the 425-nm peak (characteristic for both [2Fe-2S] and [4Fe-4S] clusters) (Fig. 5*C*). The absorption decay at 600 nm could be fitted satisfactorily by a monoexponential decay with a half-life of ~19 min (*SI Appendix*, Fig. S6*C*). This rate was similar to that recorded at 340 nm (Fig. 5*B*), and therefore indicates electron flow from NADPH to holo-ISCA1–ISCA2 in the presence of catalytic amounts of FDX2, FDXR, and IBA57. These spectral changes were specific, as they were neither observed with holo-ISCA2 as an acceptor, nor when an IBA57 mutant protein was used in which the universally conserved Cys259 was replaced by Ser (C259S) (Fig. 5*D*). Moreover, using [2Fe-2S] holo-GLRX5 instead of holo-ISCA1–ISCA2 as a potential electron acceptor did not result in a fast absorption decay at 340 nm, and the three [2Fe-2S] cluster-characteristic peaks of GLRX5 (414, 516, and 591 nm) decreased uniformly and only marginally (Fig. 5 *B* and *D* and *SI Appendix*, Fig. S6*B*). Since the difference spectrum (start minus end) was similar to the spectrum of holo-GLRX5 above 400 nm, the small changes were likely caused by cluster decomposition during the incubation (Fig. 5*C*).

As a further control, we explored whether the electron flow from NADPH to holo-ISCA–ISCA2 was mediated by IBA57 alone. Oxidized holo-ISCA1–ISCA2 was incubated with IBA57. After an initial small drop at 340 nm, only little further decease was observed at later time points (Fig. 5*B*). However, addition of catalytic amounts of FDX2 and FDXR after 50 min initiated an absorption decay at both 340 nm and 600 nm, with a half-life similar to that for the standard reaction (Fig. 5*B* and *SI Appendix*, Fig. S6*C*). Taken together, these data clearly show that holo-ISCA1–ISCA2 is the electron acceptor of FDX2. With this

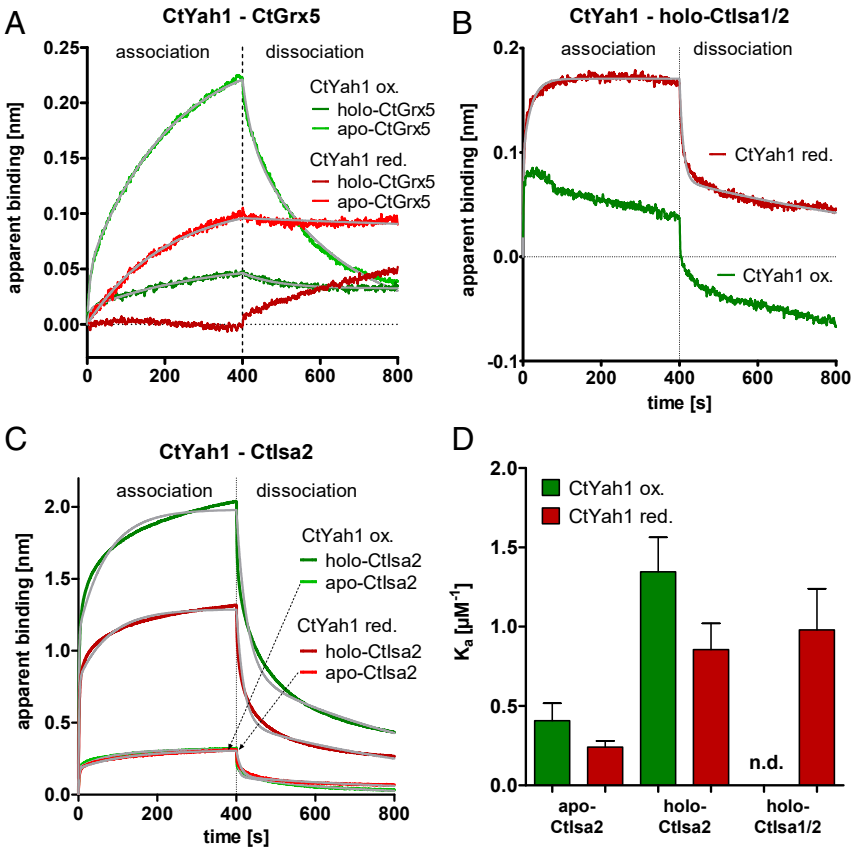

Fig. 4. Mitochondrial ferredoxin physically interacts with late-acting ISC factors. Association and dissociation time-courses were recorded for immobilized CtYah1 in its oxidized (green) and reduced form (red) with CtGrx5 (*A*), holo-Ctlsa1–Ctlsa2 (*B*), or Ctlsa2 (*C*) (each at 20-μM concentration) by BLI. Gray lines indicate fits of the data according to a 2:1 heterogeneous ligand interaction. (*D*) Dissociation constants (K_D) were derived from fits of concentration variations. The corresponding association constants ($K_a = 1/K_D$) are displayed for the indicated protein pairs. Error bars indicate the SEM ($n \geq 4$).

knowledge, we tested whether catalytic amounts of holo-ISCA1–ISCA2 were able to donate electrons further to GLRX5 to induce reductive [2Fe-2S] cluster fusion on GLRX5. Holo-ISCA1–ISCA2 (3 μM) was added to a mixture containing FDX2, FDXR, and 50 μM holo-GLRX5. Yet, these low amounts of holo-ISCA1–ISCA2 did not significantly enhance NADPH consumption (Fig. 5*B*). This finding does not indicate a role of holo-ISCA1–ISCA2 as an intermediate electron donor for GLRX5. Rather, the sum of our experiments indicates that electrons flow from FDX2 to holo-ISCA1–ISCA2 in the absence of GLRX5 and apo-aconitase as cluster donor and acceptor, respectively. This finding identifies reduced holo-ISCA1–ISCA2 as a true reaction intermediate.

We finally performed a spectroscopic analysis of the ISCA-bound Fe/S clusters to explore their changes during the electron transfer reaction. As mentioned above, the UV/Vis spectrum of holo-ISCA1–ISCA2 indicated bound [2Fe-2S] clusters (Fig. 5*A*). The Mössbauer spectra of chemically reconstituted oxidized CtIsa1–Isa2 and CtIsa2 identified an unusual Fe/S cluster species (70% intensity in CtIsa1–Isa2 and 90% in CtIsa2) with spectral characteristics that fit to neither $[2Fe\text{-}2S]^{2+}$ nor $[4Fe\text{-}4S]^{2+}$ cluster species (56) (*SI Appendix*, Fig. S7 *A* and *B*). In addition, the spectrum of CtIsa1–Isa2 (but not CtIsa2) displayed a signal for a $[4Fe\text{-}4S]^{2+}$ cluster at 25% intensity. The electron paramagnetic resonance spectrum of CtIsa2 showed signals with average g value below $g = 2$ ($g_{av} = 1.99$). These values, together with the fact that the spectra were observed up to 90 K, indicate the presence of [2Fe-2S] clusters (*SI Appendix*, Fig. S7*C*). Virtually the same was observed for human holo-ISCA1–ISCA2 (*SI Appendix*, Fig. S7*D*). Consistent with previous findings (36), all holo-ISCA species used in this study bound between four and six iron and acid labile sulfide ions per dimer (*SI Appendix*, Fig. S7*E*). Taken together, these findings indicate that the eukaryotic A-type ISC proteins can bind $[2Fe\text{-}2S]^{2+}$ clusters with an atypical Mössbauer signature and a minor fraction of $[4Fe\text{-}4S]^{2+}$ clusters at variable amounts. Therefore, the electron flow from FDX2 to holo-ISCA1–ISCA2 is used for reductive fusion of $[2Fe\text{-}2S]^{2+}$ into $[4Fe\text{-}4S]^{2+}$ clusters. This is directly seen from the UV/Vis spectral changes upon IBA57-dependent electron transfer from FDX2 (compare Fig. 5 *A* and *C*): That is, the disappearance of [2Fe-2S] clusters (loss of the 525- and 600-nm peaks) and conversion to a [4Fe-4S] species (loss and gain of absorption in the 420-nm range, the major absorption peak of [4Fe-4S] clusters).

Comparison of the ISC Dependence of Mitochondrial [2Fe-2S] and [4Fe-4S] Protein Maturation. We finally compared the ISC factor requirements of mitochondrial [4Fe-4S] protein assembly with those of [2Fe-2S] protein assembly using GLRX5 as the common cluster donor, and in particular asked whether unidentified ISC components may be required also for [2Fe-2S] cluster transfer. As target apoproteins, we used human FDX1 and the heterologous plant-type [2Fe-2S] ferredoxin from the cyanobacterium *Synechococcus elongatus* (Fd). Both apoforms were prepared by acid precipitation (57). Holo-ferredoxin formation was quantified by their ability to reduce cytochrome *c* in the presence of the cognate ferredoxin reductase and NADPH (58) (*SI Appendix*, Fig. S8). In the absence of reductants, holo-GLRX5 (present at a 2:1 ratio relative to apo-FDX1) was capable of [2Fe-2S] cluster transfer to human FDX1, yet only ~30% of the available FDX1

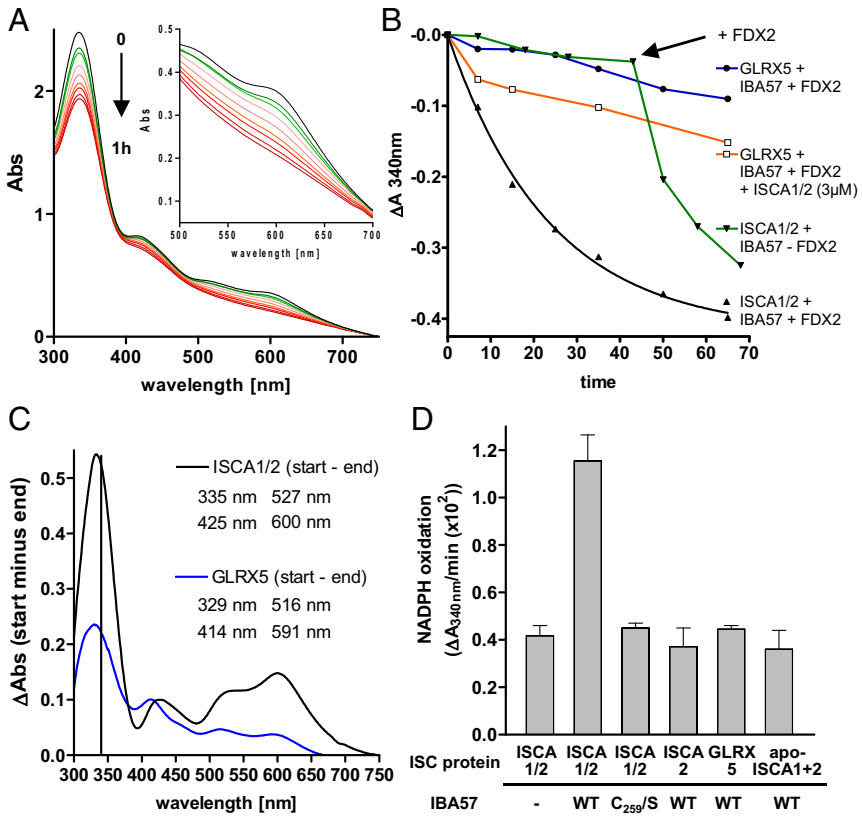

Fig. 5. FDX2 transfers electrons to holo-ISCA1–ISCA2 for IBA57-dependent [2Fe-2S] cluster fusion. (*A*) Oxidized holo-ISCA1–ISCA2 (50 μM) was mixed with 0.18 mM NADPH, 1 mM GSH, and 3 μM FDX2. UV/Vis spectra were taken in the absence of FDXR (black), 7 min (dark green), and 15 min (green) after addition of 0.5 μM FDXR. Then, 3 μM IBA57 was added and further spectra were recorded after 7 to 65 min (red; absorption decreasing with time). (*B*) Time course of the absorption decrease at 340 nm for the indicated mixtures. The black trace corresponds to a fit according to a monoexponential decay ($t_{1/2} \sim 16$ min). (*C*) Difference spectra for holo-ISCA1/2 (black) or GLRX5 (blue) at 50 μM in the presence of FDX2 and NADPH each recorded before (ISCA1/2 start; black spectrum in *A*) and 65 min after supplementation with 0.5 μM FDXR and 3 μM IBA57 (ISCA1/2 end; dark red spectrum in *A*). For GLRX5 see *SI Appendix*, Fig. S6*B*. The wavelengths of the respective absorption maxima are indicated. The vertical line indicates an absorption maximum of NADPH at 340 nm. (*D*) Rates of the absorption decay at 340 nm calculated for the 2- to 15-min range after mixing holo-ISCA1/2, holo-ISCA2, or holo-GLRX5 (50 μM each) with FDX2, FDXR, and NADPH in the presence or absence of wild-type or mutant IBA57-C259S, as indicated. Error bars indicate the SEM ($n = 3$).

was converted to its holoform (Fig. 6*A*). Transfer reached completion after 5 min. In contrast, the presence of Glrx1-GSH massively boosted the reaction, as 90% of apo-FDX1 became reconstituted within less than 15 s, the shortest time interval that could be analyzed (Fig. 6 *A* and *B*). The high transfer rate and efficiency suggest that this spontaneous transfer reaction is likely physiologically relevant and that no additional components are required.

To test the specificity of this transfer reaction, we asked whether other mitochondrial Fe/S cluster-containing ISC factors can act as direct cluster donors for mitochondrial [2Fe-2S] apoproteins. Strikingly, the holoforms of human ISCA1, ISCA2, ISCU2, and NFU1 were inefficient in transferring their Fe/S clusters to human apo-FDX1 in the presence of Glrx1-GSH (Fig. 6*C*). This finding indicates a clear specificity for GLRX5 as the cluster donor of mitochondrial [2Fe-2S] ferredoxin. This conclusion is consistent with previous in vivo observations showing that the mitochondrial ISCA, IBA57, and NFU1 proteins are not involved in [2Fe-2S] protein maturation (22–24, 29, 30).

To analyze the target specificity of the GLRX5-dependent [2Fe-2S] cluster transfer, we used the plant-type [2Fe-2S] ferredoxin (Fd). Fe/S cluster transfer from GLRX5 to this heterologous ferredoxin occurred, yet was significantly slower than that to human FDX1 (Fig. 6*D*). In the presence of Glrx1-GSH, about 60% of the available apo-Fd was reconstituted within 10 min. Moreover, the transfer efficiency dropped significantly in the absence of the reducing system. Similar to the observation made for apo-FDX1, the holoforms of the human ISC factors ISCA1, ISCA2, or ISCU2 did not support ferredoxin maturation, despite the presence of Glrx1-GSH. These results document a clear cluster donor and target apoprotein specificity for efficient and fast assembly of [2Fe-2S] FDX1.

The positive effect of the physiological Glrx1-GSH thiol-redox system on in vitro Fe/S cluster transfer from [2Fe-2S] donor to [2Fe-2S] acceptor proteins (and on that from [4Fe-4S] donor to [4Fe-4S] apoproteins) (*SI Appendix*, Fig. S1) implies an importance for thiol reduction. Thiol reduction is required on the side of the acceptor apoprotein, as apo-Fd was efficiently matured in the absence of any further additives when excessively reduced by TCEP under anaerobic conditions immediately prior to use (Fig. 6*E*). We asked whether the other important mitochondrial thiol-reducing system, namely the thioredoxin system consisting of the mitochondrial thioredoxin TRX2, its reductase Trr2, and NADPH can functionally replace the glutaredoxin/GSH system. Indeed, in the presence TRX2-Trr2-NADPH, [2Fe-2S] cluster transfer from holo-GLRX5 to apo-FDX1 or bacterial apo-Fd was as efficient as the in the presence of the Glrx1/GSH system, even when this system was complemented by its specific reductase Glr1 and NADPH (Fig. 6*F*). These findings indicate an important, yet redundant role of the two major cellular thiol-specific redox systems in apoprotein thiol reduction prior to [2Fe-2S] cluster transfer and insertion.

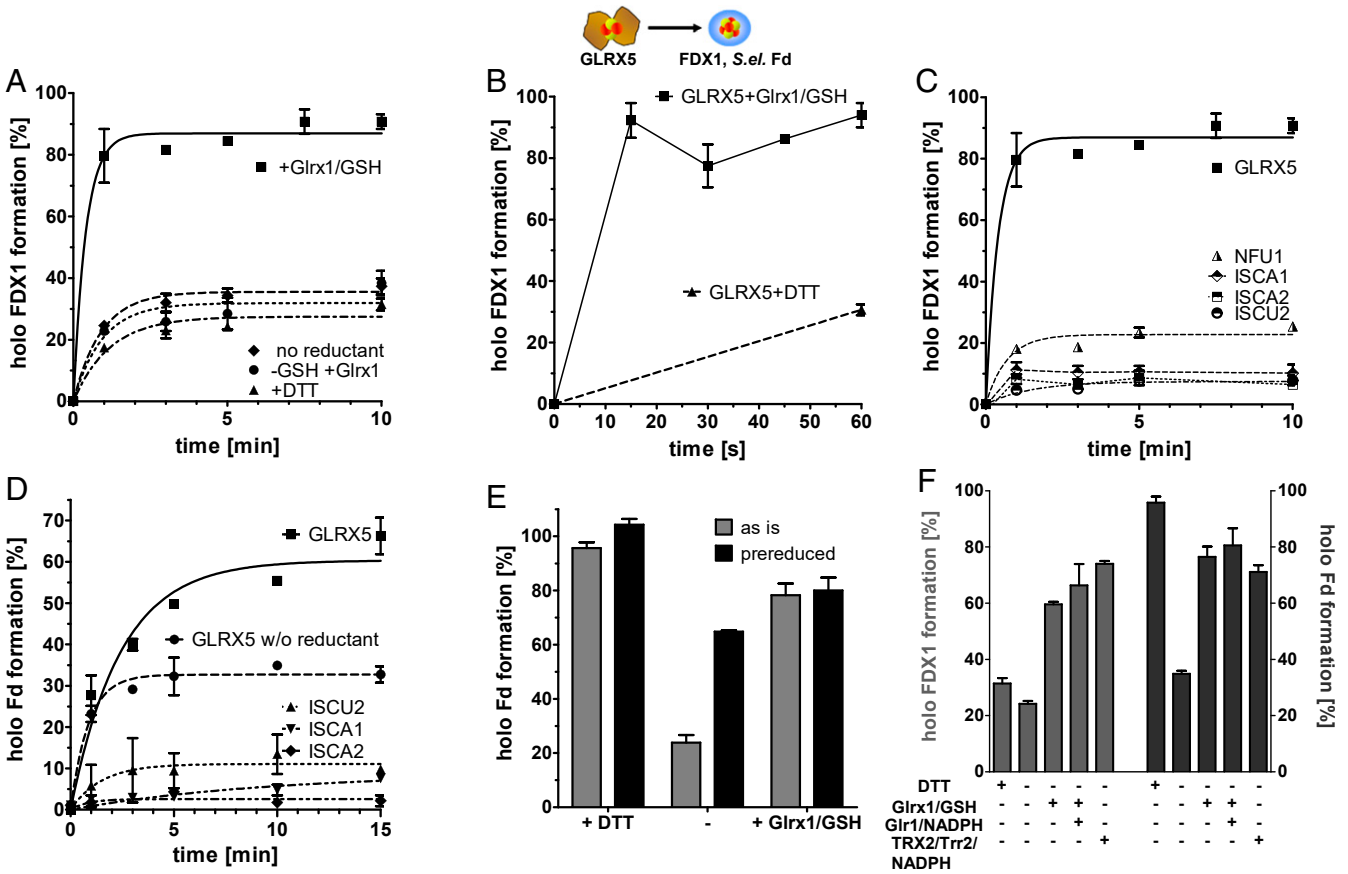

Fig. 6. Holo-GLRX5 and the glutaredoxin or thioredoxin thiol reducing systems are sufficient for rapid and efficient maturation of [2Fe-2S] ferredoxin FDX1. (*A*) Time course of the Fe/S cluster transfer from human holo-GLRX5 (50 μM) to human apo-FDX1 (25 μM) in the presence of (as indicated) 4 mM GSH and 25 μM Glrx1 (+Glrx1/GSH), 2 mM DTT, 25 μM Glrx1 without GSH, or in the absence of reductants. (*B*) Initial phase of the time course of Fe/S cluster transfer from holo-GLRX5 to apo-FDX1 as in *A*. (*C*) Fe/S cluster transfer from the indicated reconstituted human ISC holo-proteins (50 μM each) to apo-FDX1 (25 μM) in the presence of Glrx1-GSH. (*D*) Fe/S cluster transfer from the indicated reconstituted human ISC holo-proteins (50 μM each) to plant-type bacterial [2Fe-2S] apo-ferredoxin from *S. elongatus* (Fd) (25 μM) in the presence of Glrx1-GSH. A transfer reaction from GLRX5 to Fd without added reductants is included (w/o; circles). (*E*) Fe/S cluster transfer to plant-type [2Fe-2S] apo-Fd from GLRX5 (50 μM) after 10 min in the presence of 2 mM DTT, in the absence of reductants (–), or in the presence of Glrx1-GSH. Apo-Fd (25 μM) was either used as is (gray bars) or reduced anaerobically immediately prior to utilization. (*F*) Maturation of human apo-FDX1 or apo-Fd (25 μM) after 10 min incubation with holo-GLRX5 (50 μM) in the presence of the indicated components of the glutaredoxin (4 mM GSH, 25 μM Glrx1, 1 μM Glr1, 1 mM NADPH) or thioredoxin systems (5 μM TRX2, 1 μM Trr2, 1 mM NADPH). Solid lines in *A*, *C*, and *D* represent fits of the data according to a pseudo-first order kinetics; 100% activation corresponds to 25 μM holoprotein.

Discussion

We have biochemically reconstituted the final steps in the formation of mitochondrial [2Fe-2S] and [4Fe-4S] proteins and defined the minimal set of ISC factors involved. For [2Fe-2S] protein biogenesis, our experiments suggest that GLRX5 functions as the dominant physiological cluster donor in mitochondria that can rapidly transfer its transiently bound cluster without further assistance to [2Fe-2S] target apoproteins (Fig. 7). This conclusion is consistent with in vivo studies (2, 14). For maturation of mitochondrial [4Fe-4S] proteins, GLRX5 also functions as the initial cluster donor. Yet, cluster trafficking from GLRX5 and conversion into [4Fe-4S] forms essentially required the simultaneous presence of the three late-acting ISC components ISCA1, ISCA2, and IBA57, as defined earlier in vivo (22–24) (Fig. 7). Additionally, and so far unknown, the mitochondrial electron transfer chain NADPH–FDXR–FDX2 was essential for efficient and fast in vitro [4Fe-4S] protein assembly. FDX2 interacts with the ISCA1–ISCA2 heterodimer and reduces its bound $[2Fe\text{-}2S]^{2+}$ clusters. The sum of these ISC proteins represents the minimal set of components required for formation of simple mitochondrial [4Fe-4S] proteins. In special cases, this system may need additional ISC factors, such as NFU1, yet for aconitase maturation this factor seems dispensable both in vivo and in vitro. Collectively, our analyses suggest that FDX2 not only provides electrons for [2Fe-2S] cluster synthesis on the ISCU2 scaffold (8, 10), but is also necessary for reductive fusion of $[2Fe\text{-}2S]^{2+}$ to $[4Fe\text{-}4S]^{2+}$ clusters on the ISCA proteins. Due to the FDX2 requirement for [2Fe-2S] cluster synthesis in the early part of the mitochondrial ISC system (8, 9, 52), its renewed necessity for [4Fe-4S] protein biogenesis could not be disclosed by in vivo studies.

In cells, Fe/S clusters are generated on scaffold proteins, and then are handed over to various trafficking factors in a unidirectional fashion to finally become inserted into target apoproteins. In the current literature, different mitochondrial ISC proteins have been proposed as Fe/S cluster donor, transfer, or carrier proteins, on the basis that these proteins can bind Fe/S clusters in a labile, transient fashion and transfer them to downstream recipient apoproteins under appropriate in vitro conditions. Usually, these in vitro transfer reactions include the artificial reductant DTT, a cytotoxic chemical that is known to introduce artifacts in Fe/S cluster-related reactions (8, 10, 59). Most likely due to the use of this artificial reductant, and the mixed use of trafficking and acceptor proteins from different organisms and different cellular

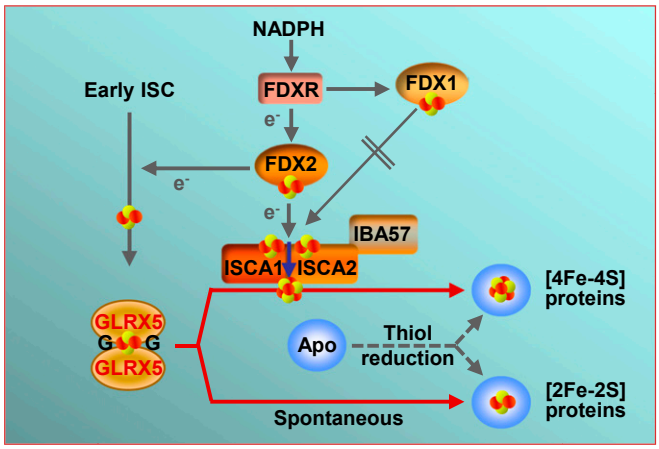

Fig. 7. Model for the biogenesis of mitochondrial [2Fe-2S] and [4Fe-4S] proteins. Dimeric monothiol glutaredoxin GLRX5 receives a glutathione (G)-bound, bridging [2Fe-2S] cluster from the early-acting ISC components (2). GLRX5 serves as a cluster donor for both [2Fe-2S] and [4Fe-4S] target apoproteins, once their cysteine thiols are reduced (e.g., by the cellular glutaredoxin or thioredoxin reduction systems) (61). Cluster transfer from GLRX5 and insertion into [2Fe-2S] target apoproteins occurs spontaneously. Dislocation of the GLRX5-bound [2Fe-2S] cluster, fusion to a [4Fe-4S] cluster and its insertion into thiol-reduced apoproteins requires ISCA1–ISCA2, IBA57, as well as the electron (e^-) transfer chain NADPH, ferredoxin reductase FDXR, and ferredoxin FDX2. The latter system catalyzes the reductive fusion of $[2Fe\text{-}2S]^{2+}$ to $[4Fe\text{-}4S]^{2+}$ clusters in a IBA57-dependent fashion (blue arrow). Despite its structural similarity, the FDX2 paralog FDX1 (also known as adrenodoxin) is not functional in this reaction.

compartments, many of the in vitro findings do not match the in vivo requirements for ISC components as determined by staging experiments following the flow of iron ions from one to another ISC protein and finally to apoproteins (see, e.g., refs. 18, 23, and 60). To closely mimic the physiological situation, our [2Fe-2S] and [4Fe-4S] cluster reconstitution systems avoided nonnatural reductants by replacing them with the physiological Glrx1-GSH thiol-redox system (61, 62).

In contrast to DTT-based reactions, our in vitro Fe/S cluster transfers in the presence of Glrx1-GSH showed several features that are in line with in vivo expectations (Fig. 7). First, human GLRX5 displayed particularly high rates of [2Fe-2S] cluster transfer to acceptor proteins from the same organism (e.g., FDX1). These were more than 50-fold higher than those to a foreign bacterial ferredoxin. This likely reflects an optimized interaction between physiological ISC donor and apoprotein acceptor pairs in a given organism. Second, Fe/S cluster transfer to human ferredoxin was considerably faster than in the presence of artificial reductants, which indicates that physiologically relevant Fe/S cluster transfer reactions may proceed much faster than the slow reduction of disulfide bonds by artificial reducing agents in vitro. Third, the comparably slow and inefficient Fe/S cluster transfer from the other Fe/S cluster-containing ISC factors ISCU2, ISCA1, ISCA2, and NFU1 in the presence of Glrx1/GSH demonstrate a striking kinetic advantage of GLRX5 that renders a primary role of these former ISC factors as Fe/S cluster donors for mitochondrial [2Fe-2S] apoproteins in the presence of GLRX5 unlikely. This conclusion is in full agreement with in vivo findings that confined the role of yeast and human ISCA1, ISCA2, and NFU1 proteins to the maturation of mitochondrial [4Fe-4S] proteins (23, 24, 29, 30). Yet, despite its role as the central [2Fe-2S] cluster donor in mitochondria, deletion of *GRX5* is not lethal in yeast (62). Under GLRX5 deficiency, [2Fe-2S] cluster transfer may occur directly from ISCU2, possibly still in collaboration with the Hsp40-Hsp70 chaperone system or other ISC transfer factors (12).

In contrast to [2Fe-2S] protein maturation, the unassisted transfer and conversion of [2Fe-2S] clusters from holo-GLRX5 to [4Fe-4S] apoproteins was inefficient, even in the presence of the physiologically relevant ISCA1–ISCA2–IBA57 proteins. The fusion of oxidized low potential $[2Fe\text{-}2S]^{2+}$ clusters on GLRX5 to an oxidized low potential $[4Fe\text{-}4S]^{2+}$ cluster for aconitase insertion formally requires the input of two electrons (45). In vitro, this reductive cluster coupling can artificially be mediated by DTT at reasonable efficiency (Fig. 1), explaining why this reductant is widely used in published [4Fe-4S] cluster assembly schemes, including those involving A-type ISC proteins as [2Fe-2S] cluster donors (see, e.g., refs. 25, 26, 28, 36, 42–44, and 63). However, none of these reactions simultaneously contained all ISCA1–ISCA2–IBA57 proteins, casting doubts that these reconstitutions reflected the correct in vivo pathway. Interestingly, the DTT function in reductive coupling of $[2Fe\text{-}2S]^{2+}$ to $[4Fe\text{-}4S]^{2+}$ clusters could not be replaced by the physiological thiol reducing systems, indicating that the primary action of DTT in this process is artificial reductive cluster fusion.

We identified the crucial role of the mitochondrial electron transfer chain NADPH–FDXR–FDX2 in reductive cluster coupling (Fig. 7). The ferredoxin function at this step is conserved in eukaryotes, as indicated by the ability of the fungal ferredoxin Yah1 from *C. thermophilum* to efficiently replace human FDX2 in our aconitase reconstitution system. Moreover, it seems likely that it is also conserved in bacteria that contain the *isc* operon encoding the [2Fe-2S] ferredoxin Fdx with close relation to Yah1-FDX2 (5). Unlike bacteria, fungi, and many unicellular eukaryotes, higher eukaryotes including man contain a second mitochondrial ferredoxin, termed FDX1, which is involved in steroid biosynthesis (8, 64). Despite its structural similarity to FDX2, FDX1 was not functional in our reconstitution system, demonstrating an impressive specificity for FDX2, a result fully consistent with earlier in vivo work (Fig. 7) (11). In other studies, FDX1 has been reported to contribute to cellular Fe/S cluster biogenesis on ISCU2, even though at much lower efficiency than FDX2 (53). Our finding that FDX1 did not support reductive coupling of $[2Fe\text{-}2S]^{+2}$ to $[4Fe\text{-}4S]^{+2}$ clusters in vitro emphasizes that FDX1 plays no important in vivo role in human Fe/S protein biogenesis.

Several results suggest that the mitochondrial NADPH–FDXR–FDX2 system functions as the sole natural source of electrons for the reductive coupling of $[2Fe\text{-}2S]^{2+}$ clusters in mitochondria. First, we saw no activation of aconitase in the presence of the GSH/glutaredoxin or thioredoxin systems instead of the NADPH–FDXR–FDX2 chain. Second, components of the mitochondrial respiratory chain can be excluded as a native electron source for the reductive coupling of $[2Fe\text{-}2S]^{2+}$ clusters, since aconitase is perfectly active in yeast cells lacking mitochondrial DNA (65). Third, ascorbic acid could not replace NADPH–FDXR–FDX2 in our assay, making it unlikely that its enantiomer D-erythroascorbic acid, synthesized in *S. cerevisiae* mitochondria as an antioxidant compound, could potentially be used for reduction (66).

Consistent with in vivo findings, the formation of [4Fe-4S] clusters on aconitase in vitro essentially required all three late-acting ISC factors ISCA1, ISCA2, and IBA57 (22–24). Hence, the observation that only ISCA1 was found to be required for [4Fe-4S] protein maturation in mouse skeletal muscle and neuronal cells is best explained by an inefficient knockdown of the corresponding mRNAs for ISCA2 and IBA57 (25). Consistent with this, pathogenic mutations in either *ISCA1*, *ISCA2*, or *IBA57* genes are associated with similar disease phenotypes that include neurodegenerative defects, clearly showing that each encoded protein is crucial in neurons (33, 34, 67, 68). Our in vitro findings further support the suggestion derived from in vivo studies that

Fe/S cluster formation on mitochondrial [4Fe-4S] proteins crucially involves the formation of a heterodimeric ISCA1–ISCA2 complex, since only a chemically coreconstituted ISCA1–ISCA2 heterodimer was functional in this process in vitro (22, 23). Single ISCA1 or ISCA2 species either reconstituted or in their apoforms were nonfunctional. Notably, the holo-ISCA1–ISCA2 heterodimer was required only in catalytic amounts, suggesting that the [4Fe-4S] cluster on ISCA1–ISCA2 is further transferred to aconitase and replaced with two [2Fe-2S] clusters from GLRX5 for a renewed fusion event.

Our work provides evidence that the holo-ISCA1–ISCA2 heterodimer receives electrons from reduced FDX2 via specific complex formation. We did not find any evidence that GLRX5 is efficiently reduced by FDX2, neither directly nor via ISCA1–ISCA2. Hence, GLRX5 is most likely not a device for reductive $[2Fe\text{-}2S]^{2+}$ cluster coupling, although monothiol glutaredoxins are in principle able to accommodate [4Fe-4S] clusters (43). Therefore, the ISCA1–ISCA2 heterodimer functions as the fusion device for the construction of a $[4Fe\text{-}4S]^{2+}$ cluster. An "assembler" function had been suggested earlier for the ISCA proteins (36), but these experiments contained 5 mM DTT, which artificially replaced the function of FDX2. Strikingly, these experiments lacked IBA57, which we found to be essential for FDX2-mediated reductive Fe/S cluster coupling. The mutant IBA57-Cys259S protein was nonfunctional, suggesting that this conserved Cys residue plays a decisive catalytic role in cluster fusion that now can be defined more precisely. IBA57 could additionally be involved in facilitating the transfer of the [4Fe-4S] cluster from ISCA1–ISCA2 to target proteins, since deletion of yeast *IBA57* leads to iron accumulation on Isa1–Isa2 (23). Our reconstitution system provides an excellent experimental set-up to address these interesting mechanistic details.

Materials and Methods

Fe/S Cluster Transfer Assays. Recombinant proteins were expressed in *Escherichia coli*, as described previously (69) (*SI Appendix*, Table S2). Chemical reconstitution of Fe/S proteins was carried out as described previously (69) (*SI Appendix, SI Materials and Methods*). Fe/S donor proteins were mixed at 50-μM final concentration (25 μM for holo-NFU1) with apo-Fd or apo-FDX1 at 25 μM or Leu1 and ACO2 at 20 μM final concentrations in transfer buffer (50 mM Tris·HCl, pH 8.0, 150 mM NaCl, 5% glycerol). Where indicated, reactions were supplemented with 5 μM IBA57, 5 μM holo-ISCA1–ISCA2, 1 μM FDXR, 1 μM FDX2 (or FDX1), 1 mM NADPH, 1 mM $MgCl_2$ and, when indicated, with 5 μM apo-NFU1. Where indicated, reactions were further supplemented with either 4 mM GSH 25 μM Glrx1, 5 μM TRX2 plus 0.5 μM Trr2 plus 1 mM NADPH, 2 mM DTT, 4 mM TCEP, or 4 mM mercaptoethanol. At the indicated time points, 4- to- 5-μL aliquots were withdrawn and analyzed for ACO2 or Leu1 enzyme activities (55) or for ferredoxin assembly assayed by cytochrome *c* reduction activity (58) (*SI Appendix*, Fig. S8).

Capture-Based BLI. Bimolecular interactions were measured in an Octet K2 Instrument (Molecular Devices) using supersteptavidin sensors loaded with biotinylated CtYah1. For background correction, binding studies were carried out in parallel with an empty sensor. For K_D determinations, concentration variations of the partner protein were carried out. Data were fitted according to a 2:1 heterogeneous ligand model using Octet Data Analysis HT10.0 software (for details, see *SI Appendix, Materials and Methods* and Figs. S3–S5).

Miscellaneous Methods. Statistical analyses were carried out using GraphPad Prism. Errors bars indicate the SEM ($n \geq 3$). Panels in Figs. 1, 3, and 5 display data of representative experimental sets each carried out in parallel on the same day. The following published methods were used: Manipulation of DNA and PCR (70), transformation of yeast cells (71), preparation of yeast mitochondria (72), and immunological techniques (73). For further details, see *SI Appendix, Materials and Methods*.

Data Availability. Associated protocols and materials are found *SI Appendix, SI Materials and Methods*. Original spectroscopic data are available at Open Science Framework (https://osf.io/tbkr9/?view_only=e38759d63b2d47e79c8a2c2ec5ee0766).

ACKNOWLEDGMENTS. We thank Drs. Carsten Berndt and Nicolas Rouhier for providing plasmids. This work was supported by the Deutsche Forschungsgemeinschaft (SFB 987, SPP 1710, and SPP 1927). We acknowledge the contribution of the Core Facility 'Protein Biochemistry and Spectroscopy' of Philipps-Universität Marburg and networking support from the COST Action FeSBioNet (Contract CA15133).

1. P. Zanello, Structure and electrochemistry of proteins harboring iron-sulfur clusters of different nuclearities. Part IV. Canonical, non-canonical and hybrid iron-sulfur proteins. *J. Struct. Biol.* **205**, 103–120 (2019).
2. R. Lill, S. A. Freibert, Mechanisms of mitochondrial iron-sulfur protein biogenesis. *Annu. Rev. Biochem.* **89**, 471–499 (2020).
3. N. Maio, A. Jain, T. A. Rouault, Mammalian iron-sulfur cluster biogenesis: Recent insights into the roles of frataxin, acyl carrier protein and ATPase-mediated transfer to recipient proteins. *Curr. Opin. Chem. Biol.* **55**, 34–44 (2020).
4. S. Ciofi-Baffoni, V. Nasta, L. Banci, Protein networks in the maturation of human iron-sulfur proteins. *Metallomics* **10**, 49–72 (2018).
5. B. Py, F. Barras, Genetic approaches of the Fe-S cluster biogenesis process in bacteria: Historical account, methodological aspects and future challenges. *Biochim. Biophys. Acta* **1853**, 1429–1435 (2015).
6. J. Przybyla-Toscano, M. Roland, F. Gaymard, J. Couturier, N. Rouhier, Roles and maturation of iron-sulfur proteins in plastids. *J. Biol. Inorg. Chem.* **23**, 545–566 (2018).
7. V. D. Paul, R. Lill, Biogenesis of cytosolic and nuclear iron-sulfur proteins and their role in genome stability. *Biochim. Biophys. Acta* **1853**, 1528–1539 (2015).
8. H. Webert *et al.*, Functional reconstitution of mitochondrial Fe/S cluster synthesis on Isu1 reveals the involvement of ferredoxin. *Nat. Commun.* **5**, 5013 (2014).
9. M. T. Boniecki, S. A. Freibert, U. Mühlenhoff, R. Lill, M. Cygler, Structure and functional dynamics of the mitochondrial Fe/S cluster synthesis complex. *Nat. Commun.* **8**, 1287 (2017).
10. S. Gervason *et al.*, Physiologically relevant reconstitution of iron-sulfur cluster biosynthesis uncovers persulfide-processing functions of ferredoxin-2 and frataxin. *Nat. Commun.* **10**, 3566 (2019).
11. A. D. Sheftel *et al.*, Humans possess two mitochondrial ferredoxins, Fdx1 and Fdx2, with distinct roles in steroidogenesis, heme, and Fe/S cluster biosynthesis. *Proc. Natl. Acad. Sci. U.S.A.* **107**, 11775–11780 (2010).
12. H. H. Kampinga, E. A. Craig, The HSP70 chaperone machinery: J proteins as drivers of functional specificity. *Nat. Rev. Mol. Cell Biol.* **11**, 579–592 (2010).
13. C. Berndt, C. H. Lillig, Glutathione, glutaredoxins, and iron. *Antioxid. Redox Signal.* **27**, 1235–1251 (2017).
14. J. Couturier, J. Przybyla-Toscano, T. Roret, C. Didierjean, N. Rouhier, The roles of glutaredoxins ligating Fe-S clusters: Sensing, transfer or repair functions? *Biochim. Biophys. Acta* **1853**, 1513–1527 (2015).
15. L. Banci *et al.*, [2Fe-2S] cluster transfer in iron-sulfur protein biogenesis. *Proc. Natl. Acad. Sci. U.S.A.* **111**, 6203–6208 (2014).
16. C. Johansson *et al.*, The crystal structure of human GLRX5: Iron-sulfur cluster coordination, tetrameric assembly and monomer activity. *Biochem. J.* **433**, 303–311 (2011).
17. M. T. Rodríguez-Manzaneque, J. Tamarit, G. Bellí, J. Ros, E. Herrero, Grx5 is a mitochondrial glutaredoxin required for the activity of iron/sulfur enzymes. *Mol. Biol. Cell* **13**, 1109–1121 (2002).
18. U. Mühlenhoff, J. Gerber, N. Richhardt, R. Lill, Components involved in assembly and dislocation of iron-sulfur clusters on the scaffold protein Isu1p. *EMBO J.* **22**, 4815–4825 (2003).
19. R. A. Wingert *et al.*; Tübingen 2000 Screen Consortium, Deficiency of glutaredoxin 5 reveals Fe-S clusters are required for vertebrate haem synthesis. *Nature* **436**, 1035–1039 (2005). Correction in: *Nature* **437**, 920 (2005).
20. C. Camaschella *et al.*, The human counterpart of zebrafish shiraz shows sideroblastic-like microcytic anemia and iron overload. *Blood* **110**, 1353–1358 (2007).
21. H. Ye *et al.*, Glutaredoxin 5 deficiency causes sideroblastic anemia by specifically impairing heme biosynthesis and depleting cytosolic iron in human erythroblasts. *J. Clin. Invest.* **120**, 1749–1761 (2010).
22. C. Gelling, I. W. Dawes, N. Richhardt, R. Lill, U. Mühlenhoff, Mitochondrial Iba57p is required for Fe/S cluster formation on aconitase and activation of radical SAM enzymes. *Mol. Cell. Biol.* **28**, 1851–1861 (2008).
23. U. Mühlenhoff, N. Richter, O. Pines, A. J. Pierik, R. Lill, Specialized function of yeast Isa1 and Isa2 proteins in the maturation of mitochondrial [4Fe-4S] proteins. *J. Biol. Chem.* **286**, 41205–41216 (2011).
24. A. D. Sheftel *et al.*, The human mitochondrial ISCA1, ISCA2, and IBA57 proteins are required for [4Fe-4S] protein maturation. *Mol. Biol. Cell* **23**, 1157–1166 (2012).
25. L. K. Beilschmidt *et al.*, ISCA1 is essential for mitochondrial Fe_4S_4 biogenesis in vivo. *Nat. Commun.* **8**, 15124 (2017).
26. S. Gourdoupis, V. Nasta, V. Calderone, S. Ciofi-Baffoni, L. Banci, IBA57 recruits ISCA2 to form a [2Fe-2S] cluster-mediated complex. *J. Am. Chem. Soc.* **140**, 14401–14412 (2018).
27. V. Nasta *et al.*, Structural properties of [2Fe-2S] ISCA2-IBA57: A complex of the mitochondrial iron-sulfur cluster assembly machinery. *Sci. Rep.* **9**, 18986 (2019).
28. V. Nasta, D. Suraci, S. Gourdoupis, S. Ciofi-Baffoni, L. Banci, A pathway for assembling $[4Fe\text{-}4S]^{2+}$ clusters in mitochondrial iron-sulfur protein biogenesis. *FEBS J.* **287**, 2312–2327 (2020).
29. A. Navarro-Sastre *et al.*, A fatal mitochondrial disease is associated with defective NFU1 function in the maturation of a subset of mitochondrial Fe-S proteins. *Am. J. Hum. Genet.* **89**, 656–667 (2011).

30. J. M. Cameron *et al*., Mutations in iron-sulfur cluster scaffold genes NFU1 and BOLA3 cause a fatal deficiency of multiple respiratory chain and 2-oxoacid dehydrogenase enzymes. *Am. J. Hum. Genet.* **89**, 486–495 (2011).
31. N. Ajit Bolar *et al*., Mutation of the iron-sulfur cluster assembly gene IBA57 causes severe myopathy and encephalopathy. *Hum. Mol. Genet.* **22**, 2590–2602 (2013).
32. Z. N. Al-Hassnan *et al*., ISCA2 mutation causes infantile neurodegenerative mitochondrial disorder. *J. Med. Genet.* **52**, 186–194 (2015).
33. A. Torraco *et al*., ISCA1 mutation in A patient with infantile-onset leukodystrophy causes defects in mitochondrial [4Fe-4S] proteins. *Hum. Mol. Genet.* **27**, 3650 (2018).
34. O. Stehling, V. D. Paul, J. Bergmann, S. Basu, R. Lill, Biochemical analyses of human iron-sulfur protein biogenesis and of related diseases. *Methods Enzymol.* **599**, 227–263 (2018).
35. K. D. Kim, W. H. Chung, H. J. Kim, K. C. Lee, J. H. Roe, Monothiol glutaredoxin Grx5 interacts with Fe-S scaffold proteins Isa1 and Isa2 and supports Fe-S assembly and DNA integrity in mitochondria of fission yeast. *Biochem. Biophys. Res. Commun.* **392**, 467–472 (2010).
36. D. Brancaccio *et al*., Formation of [4Fe-4S] clusters in the mitochondrial iron-sulfur cluster assembly machinery. *J. Am. Chem. Soc.* **136**, 16240–16250 (2014).
37. B. Roche *et al*., Iron/sulfur proteins biogenesis in prokaryotes: Formation, regulation and diversity. *Biochim. Biophys. Acta* **1827**, 455–469 (2013).
38. C. Wachnowsky, I. Fidai, J. A. Cowan, Iron-sulfur cluster biosynthesis and trafficking—Impact on human disease conditions. *Metallomics* **10**, 9–29 (2018).
39. J. J. Braymer, R. Lill, Iron-sulfur cluster biogenesis and trafficking in mitochondria. *J. Biol. Chem.* **292**, 12754–12763 (2017).
40. B. Py *et al*., Molecular organization, biochemical function, cellular role and evolution of NfuA, an atypical Fe-S carrier. *Mol. Microbiol.* **86**, 155–171 (2012).
41. D. T. Mapolelo, B. Zhang, S. G. Naik, B. H. Huynh, M. K. Johnson, Spectroscopic and functional characterization of iron-bound forms of Azotobacter vinelandii (Nif)IscA. *Biochemistry* **51**, 8056–8070 (2012).
42. H. Gao *et al*., Arabidopsis thaliana Nfu2 accommodates [2Fe-2S] or [4Fe-4S] clusters and is competent for in vitro maturation of chloroplast [2Fe-2S] and [4Fe-4S] cluster-containing proteins. *Biochemistry* **52**, 6633–6645 (2013).
43. B. Zhang *et al*., Monothiol glutaredoxins can bind linear [Fe3S4]+ and [Fe4S4]2+ clusters in addition to [Fe2S2]2+ clusters: Spectroscopic characterization and functional implications. *J. Am. Chem. Soc.* **135**, 15153–15164 (2013).
44. M. C. Unciuleac *et al*., In vitro activation of apo-aconitase using a [4Fe-4S] cluster-loaded form of the IscU [Fe-S] cluster scaffolding protein. *Biochemistry* **46**, 6812–6821 (2007).
45. K. Chandramouli *et al*., Formation and properties of [4Fe-4S] clusters on the IscU scaffold protein. *Biochemistry* **46**, 6804–6811 (2007).
46. B. Schilke, C. Voisine, H. Beinert, E. Craig, Evidence for a conserved system for iron metabolism in the mitochondria of Saccharomyces cerevisiae. *Proc. Natl. Acad. Sci. U.S.A.* **96**, 10206–10211 (1999).
47. A. Melber *et al*., Role of Nfu1 and Bol3 in iron-sulfur cluster transfer to mitochondrial clients. *eLife* **5**, e15991 (2016).
48. M. A. Uzarska *et al*., Mitochondrial Bol1 and Bol3 function as assembly factors for specific iron-sulfur proteins. *eLife* **5**, e16673 (2016).
49. K. Cai *et al*., Structural/functional properties of human NFU1, an intermediate [4Fe-4S] carrier in human mitochondrial iron-sulfur cluster biogenesis. *Structure* **24**, 2080–2091 (2016).
50. C. Wachnowsky, Y. Liu, T. Yoon, J. A. Cowan, Regulation of human Nfu activity in Fe-S cluster delivery-characterization of the interaction between Nfu and the HSPA9/Hsc20 chaperone complex. *FEBS J.* **285**, 391–410 (2018).
51. S. Bandyopadhyay *et al*., A proposed role for the Azotobacter vinelandii NfuA protein as an intermediate iron-sulfur cluster carrier. *J. Biol. Chem.* **283**, 14092–14099 (2008).
52. H. Lange, A. Kaut, G. Kispal, R. Lill, A mitochondrial ferredoxin is essential for biogenesis of cellular iron-sulfur proteins. *Proc. Natl. Acad. Sci. U.S.A.* **97**, 1050–1055 (2000).
53. Y. Shi, M. Ghosh, G. Kovtunovych, D. R. Crooks, T. A. Rouault, Both human ferredoxins 1 and 2 and ferredoxin reductase are important for iron-sulfur cluster biogenesis. *Biochim. Biophys. Acta* **1823**, 484–492 (2012).
54. M. C. Kennedy, M. H. Emptage, J. L. Dreyer, H. Beinert, The role of iron in the activation-inactivation of aconitase. *J. Biol. Chem.* **258**, 11098–11105 (1983).
55. S. Molik, R. Lill, U. Mühlenhoff, Methods for studying iron metabolism in yeast mitochondria. *Methods Cell Biol.* **80**, 261–280 (2007).
56. M. E. Pandelia, N. D. Lanz, S. J. Booker, C. Krebs, Mössbauer spectroscopy of Fe/S proteins. *Biochim. Biophys. Acta* **1853**, 1395–1405 (2015).
57. J. Meyer, J. M. Moulis, M. Lutz, High-yield chemical assembly of [2Fe-2X] (X = S, Se) clusters into spinach apoferredoxin: Product characterisation by Raman spectroscopy. *Biochim. Biophys. Acta* **871**, 243–249 (1986).
58. G. Forti, E. M. Meyer, Effect of pyrophosphate on photosynthetic electron transport reactions. *Plant Physiol.* **44**, 1511–1514 (1969).
59. J. Bridwell-Rabb, N. G. Fox, C. L. Tsai, A. M. Winn, D. P. Barondeau, Human frataxin activates Fe-S cluster biosynthesis by facilitating sulfur transfer chemistry. *Biochemistry* **53**, 4904–4913 (2014).
60. M. A. Uzarska, R. Dutkiewicz, S. A. Freibert, R. Lill, U. Mühlenhoff, The mitochondrial Hsp70 chaperone Ssq1 facilitates Fe/S cluster transfer from Isu1 to Grx5 by complex formation. *Mol. Biol. Cell* **24**, 1830–1841 (2013).
61. J. P. Jacquot, M. Zaffagnini, Thioredoxin and glutaredoxin systems antioxidants special issue. *Antioxidants* **8**, E68 (2019).
62. E. Herrero, G. Bellí, C. Casa, Structural and functional diversity of glutaredoxins in yeast. *Curr. Protein Pept. Sci.* **11**, 659–668 (2010).
63. D. T. Mapolelo, B. Zhang, S. G. Naik, B. H. Huynh, M. K. Johnson, Spectroscopic and functional characterization of iron-sulfur cluster-bound forms of Azotobacter vinelandii (Nif)IscA. *Biochemistry* **51**, 8071–8084 (2012).
64. P. Zanello, The competition between chemistry and biology in assembling iron-sulfur derivatives. Molecular structures and electrochemistry. Part II. {[Fe2S2](S-Cys(gamma))(4)} proteins. *Coord. Chem. Rev.* **280**, 54–83 (2014).
65. E. M. Froschauer *et al*., The mitochondrial carrier Rim2 co-imports pyrimidine nucleotides and iron. *Biochem. J.* **455**, 57–65 (2013).
66. W. K. Huh *et al*., D-Erythroascorbic acid is an important antioxidant molecule in Saccharomyces cerevisiae. *Mol. Microbiol.* **30**, 895–903 (1998).
67. J. T. Alaimo *et al*., Loss-of-function mutations in ISCA2 disrupt 4Fe-4S cluster machinery and cause a fatal leukodystrophy with hyperglycinemia and mtDNA depletion. *Hum. Mutat.* **39**, 537–549 (2018).
68. A. Lossos *et al*., Fe/S protein assembly gene IBA57 mutation causes hereditary spastic paraplegia. *Neurology* **84**, 659–667 (2015).
69. S. A. Freibert *et al*., Biochemical reconstitution and spectroscopic analysis of iron-sulfur proteins. *Methods Enzymol.* **599**, 197–226 (2018).
70. J. Sambrook, D. W. Russel, *Molecular Cloning—A Laboratory Manual*, (CSH Laboratory Press, Cold Spring Harbor, NY, ed. 3, 2001).
71. R. D. Gietz, R. A. Woods, Transformation of yeast by lithium acetate/single-stranded carrier DNA/polyethylene glycol method. *Methods Enzymol.* **350**, 87–96 (2002).
72. K. Diekert, A. I. de Kroon, G. Kispal, R. Lill, Isolation and subfractionation of mitochondria from the yeast Saccharomyces cerevisiae. *Methods Cell Biol.* **65**, 37–51 (2001).
73. E. A. Greenfield, *Antibodies—A Laboratory Manual*, (CSH Laboratory Press, Cold Spring Harbor, NY, ed. 2, 2014).